Forecasting Seismicity, Stability and Stress in Underground Mining

Stephan Arndt

Coffey Mining

Abstract: Simulation methods used in open pit and underground mining have evolved from simple stress analysis to forecasting tools providing realistic simulation for challenging geomechanics problems. Whilst simulations with in-elastic constitutive models, very detailed 3D models and life-of-mine analysis scenarios spanning decades become less limited by the growing availability of computer resources, more emphasis is given to the determination of model and material parameters. The main input parameters that can be obtained from testing are rock mass strength and in-situ stress. Tri-axial rock mass testing of samples under varying confinement pressure can be used to obtain parameters for in-elastic strain softening behaviour for a Mohr-Coulomb constitutive model. Various methods exist for the determination of the in-situ stress, divided into those that require access to the location of measurement, typically associated with higher costs, and those performed on core obtained from drill holes. Ideally there is a balance between testing and simulation that ensures an efficient approach, where value for the industry lies in the predictive capability of the simulation even before data for calibration and back-analysis becomes available. Examples using Abaqus in this paper show applications including stability, stress and seismicity in planned and operating underground mining projects.

Keywords: Mining, Underground Mining, Rock Mass Plasticity, Mine-scale Models, Mohr-Coulomb, Life-of-mine, In-situ Stress, Seismicity.

1. Introduction

Simulation in mining geomechanics aims at developing a complex mine scale model that can be calibrated against field data and achieve forecasting confidence. A combination of solutions is required to achieve this:

- **Abaqus/Standard** is used as an efficient tool to solve the equilibrium state for a three-dimensional stress field. Input data from stress measurements is often limited and analytical solutions cannot account for the topography or complexity of geological units. The resulting stress field solution can be imported in Abaqus/Explicit either by mapping the solution or using the same mesh (element-by-element assignment of initial stress).
- **Abaqus/Explicit** is used for mine-scale simulation, as it allows extreme model sizes (typically measured in tens-of-millions degrees of freedom, DOF's) whilst at the same time providing a robust solver for the highly non-linear behavior of rock mass, including strain-softening Mohr-Coulomb plasticity.
- **C3D10M tetrahedral volume elements** (ten-node tetrahedra) are essential to achieve high quality results resolution for stress and deformation within the practical limitation of

twenty to thirty million degrees of freedom (DOFs) in a mine-scale analysis. This is driven by the necessity to use tet-meshes to implement the complex geometry features that are required to capture realistic behaviour.

- **COH3D6 cohesive elements** represent the discontinuous character of the faults and lithological contacts. Cohesive elements allow large strains and large displacements with a defined constitutive thickness whilst zero geometric thickness allows easy placement inside the mesh. Taking advantage of the bi-linear fit on the shape functions of the C3D10M, four COH3D6 are placed on each pairing of element faces between volume elements.
- **The parallel solver**, commonly used with 24 CPUs in Coffey Mining, allows analysis turn-around times of 24h-48h for very large models. Running dedicated workstations for this task using 64-Bit Linux proved a reliable resource with the current uptime exceeding 600 days.
- **Python scripting,** based on a library centered on a mesh() class developed in Coffey Mining, that allows to quickly perform complex operations on mesh objects, elements, nodes, sets and input files. Other applications include using the odbAccess module for results extraction and automated image generation in Abaqus/Viewer.

Mining examples shown in the series of this conference include (Arndt, 2011), (Arndt, 2009).

2. Fitting in-situ stress to stress measurements

In a mountainous region the in-situ stress in the vicinity of an underground mine can be greatly influenced by the topography of the mine setting. This presents a challenge to provide a field solution for the equilibrium state in a Finite Element Analysis of a mine-scale problem, as the competing effects of locked-in stresses from the continental plate, the local folding and potential volcanic activities and the geometry of the topography itself can create an exceedingly complex stress distribution.

Results and interpretation for mine design purposes using the subsequent analysis of a mine-scale model can vary significantly depending on the stress field input, making this one of the most important input parameters in the modeling process.

2.1 Finite element model

The model shown in Figure 1, spanning 4km x 4km, centered on a site situated in a steep valley between ridges located more than five hundred meters above the valley floor, is used to perform the equilibrium analysis. In this contour plot only the magnitude of major principal stress is shown on a vertical cut plane through the location of the stress measurements. The valley experiences elevated stress immediately below the surface. The stress magnitude is converging to the lower, vertically linear, trend several hundred meters below surface. At the same time the principal stress directions are rotated due to geometric effects.

A similar application in reservoir geomechanics has been described by (Van Der Zee, 2011).

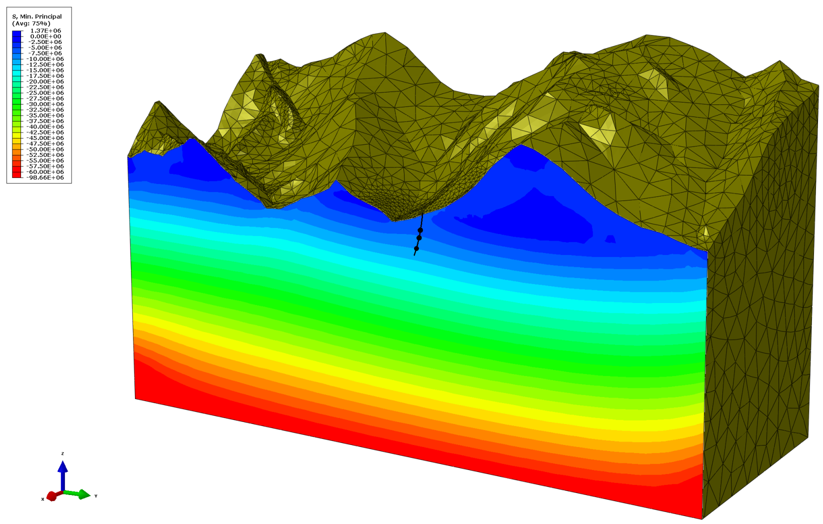

Figure 1. In-situ stress fitted to DRA measurements (points).

2.2 Stress measurements and iterative parameter fit

Using deformation rate analysis (DRA), several core sample specimens were tested to determine the stress field at the mine site. In an iterative process, performed manually, the input parameters for an analytical stress definition depending on the vertical (z) coordinate only, were adjusted to approximate the measured stress state. Admittedly, automated procedures for parameter optimization, as routinely used in other industries, would be applicable here. Given the variability often seen in stress measurements for underground mining priority would be given to either requesting more data before advanced methods are employed, but often more value can be gained from the analysis of alternative stress scenarios and the implications for the mine design.

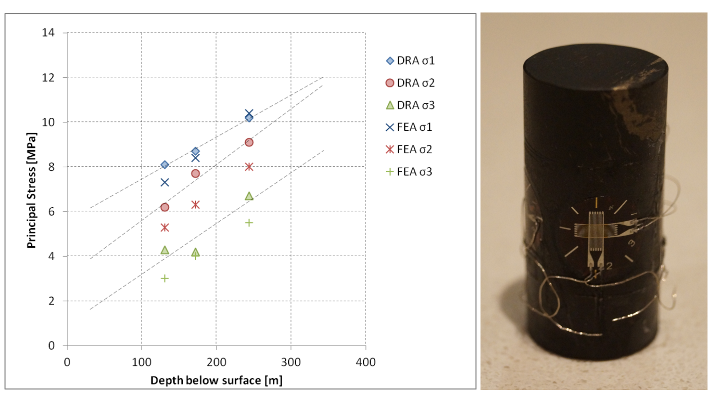

Figure 2. In-situ stress values from FEA and DRA (left), DRA specimen (right).

3. Forecasting seismicity

This example from an underground mine in Western Australia is comprised of a number of distinctively separated orebodies. These are extracted using the sub-level open stoping (SLOS) mining method; currently mining is carried out about 1000m below ground level. Mining at such depths presents certain concerns, as the horizontal stresses in this region can exceed the vertical stress significantly. The major principal stress at this depth can be as high as 80MPa, compared to 30MPa acting in the vertical direction.

3.1 Modeling approach

To be able to predict future stress conditions in a non-linear problem, the stress path that the material has experienced needs to be reproduced including the historic mining sequence to the state the mine presents itself with the currently existing voids. A non-linear constitutive model, strain-softening Mohr-Coulomb rock mass plasticity, was used with the parameters based on the tri-axial test data. Model calibration assisted in bracketing input parameters and to provide a link between the number of seismic events and the total energy release predicted by modelling.

3.2 Rock mass properties

An extensive programme of tri-axial lab testing was performed using confinement pressures ranging from 0 MPa to above 30 MPa to account for various stress conditions in the mine. Contrary to the virgin stress mentioned above, the confinement in current mining fronts would typically have dropped to values inside this range by introducing access development and by mining adjacent stopes. The Mohr-Coulomb (MC) parameters for peak and residual strengths of the rock mass were then determined from the test data.

Steps to obtain the input parameters were as follows:

1. Filtering the tri-axial test results suitable for MC envelope fitting, rejecting tests that clearly showed a shear failure along a discontinuity;
2. Construction of a MC strength envelope for the expected range of confinement stress $\sigma 3$. As the variation from five or less tests can be large, bracketing parameters based on GSI values can aid in the process. The software RocData (RocScience) was used in this step.
3. Adjustment of cohesion and Young's modulus for all materials to account for the effective behaviour on the scale of the model, where typical element sizes range from 1m to 15m in mining areas compared to specimen sizes of 18mm;
4. Defining the strain softening curve (transition from peak to residual) based on the brittle characteristics, typically over the range of 0.5% to 2.5% in-elastic strain. A vertical drop from peak to residual strength (typical behaviour of brittle high modulus rocks at low confinement) seen in tests should be avoided in the input definition to avoid problems regarding numerical stability.

The summary of input model parameters is presented in Table 1.

Table 1. Examples of model input parameters for MC for different rock mass.

Rock Type	Density (kg/m3)	Modulus E (MPa)	Poisson's ratio (-)	Cohesion (MPa)	Cohesion, res.(MPa)	Friction angle ()	Dilation angle ()
A	2826	16,600	0.31	7.2	4.2	40	13
B	2747	16,800	0.28	4.9	1.6	29	10
C	2820	25,300	0.33	15.5	7.0	40	13
D	2767	23,500	0.25	13.7	9.0	41	14
E	2674	21,300	0.24	11.7	8.2	44	15

3.3 Model construction

Due to the complexity of the mine geometry with multiple orebodies, volcanic intrusives, extensive faults and sheared lithological contacts, construction of a very detailed 3D model was required with many features defined explicitly in the finite element mesh. The complete mine-scale model had a footprint of 4km by 4km, consisting of more than 2 million elements.

Tetrahedral volume elements of type C3D10M were used together with cohesive elements of type COH3D6 to represent the discontinuous character of the faults and lithological contacts. The stope extraction sequence (also allowing for backfill of the stopes) was simulated in monthly to quarterly intervals.

To capture the area of interest with a more detailed resolution, a sub-model for the part of the orebody under investigation, spanning 600m, was built with a refined mesh, again containing about 2 million elements. The mesh for this model is shown in Figure 3. Sub-modelling requires the global model to provide boundary conditions at each mining step and the extraction sequence to be identical between both models.

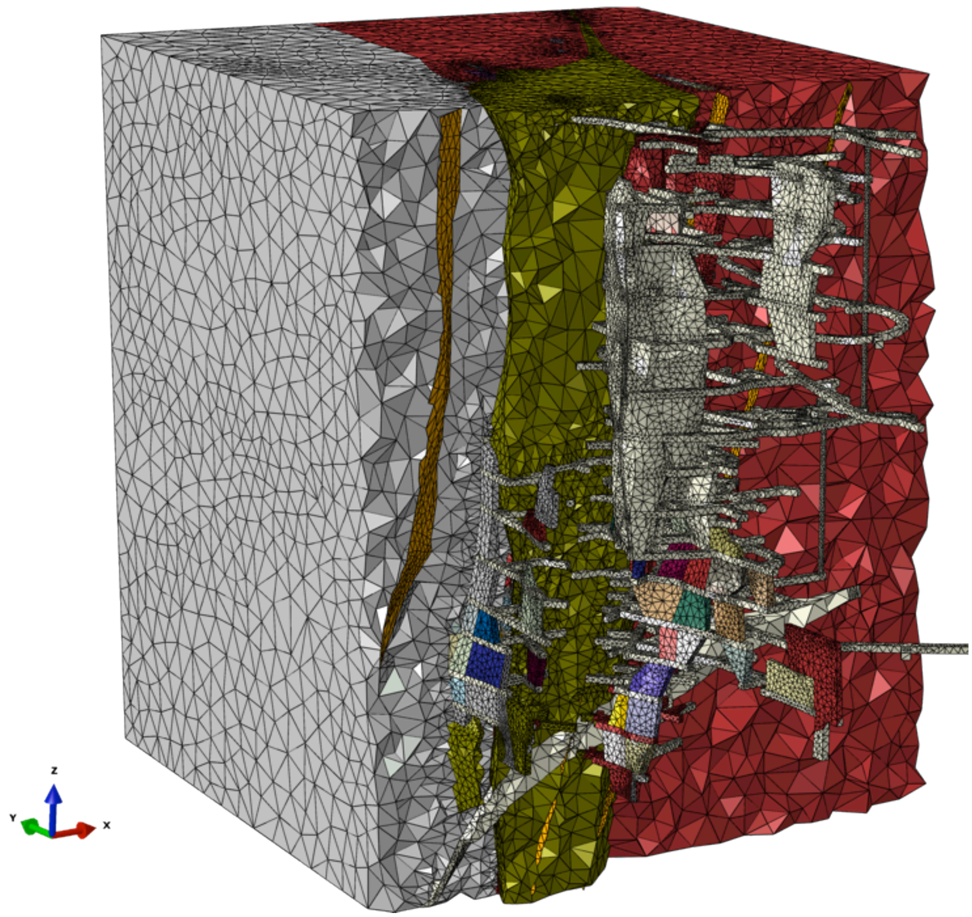

Figure 3. Sub-model of the mine showing a cut-away finite element mesh.

3.4 Calibration of seismicity with energy release

The energy theoretically available to be released due to seismicity is a combination of two components: the total strain energy and the dissipated plastic energy from rock mass yield. An example of the observed relationship between energy release in a model step and seismic events is shown below. Seismic events recorded within one month are presented as 3D spheres, with both diameter and colour scale indicating event size and the modelled energy release (Figure 4). The data shows good correlation with the events cluster observed (Figure 5).

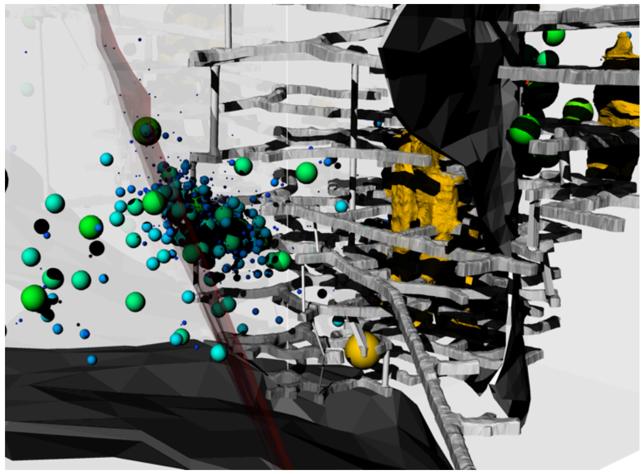

Figure 4. Seismic events contained between development and intrusive rock.

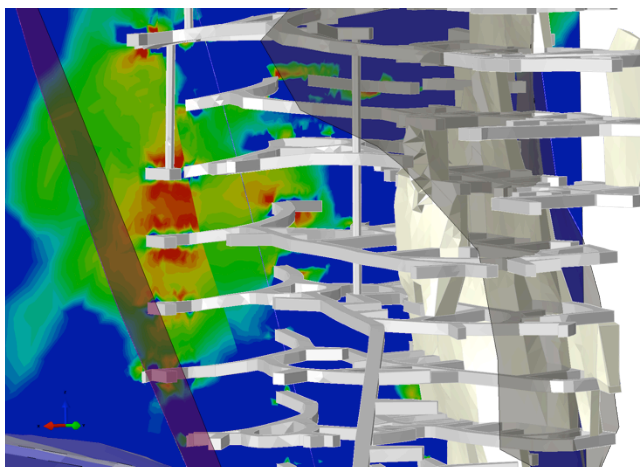

Figure 5. Energy release contours shown in a vertical section.

To quantify the calibration, a cell test approach was used with a 25m spacing of cubic cells across the orebody. For each cell in a grid of 10x10x10 cells spanning 250m in each direction (Figure 6) the number of seismic events is recorded for each monthly step. This number of events, together with the average event size, is compared to the energy release in the model for the same step. The data points for all cells and all model steps provided the basis for calibration.

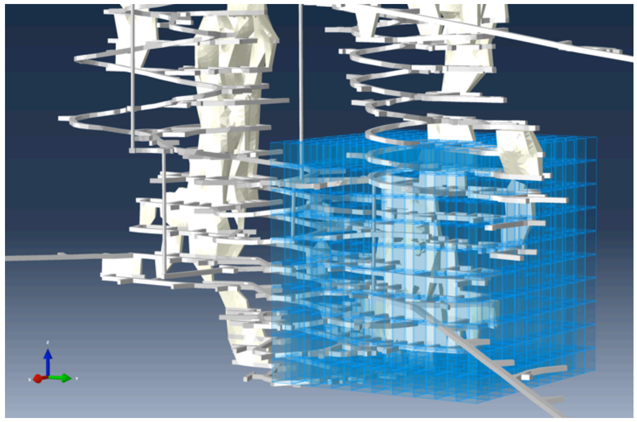

Figure 6. Grid for evaluation of seismic event numbers and model energy release

Grouped in bins of 10kJ/m^3 of energy release, average numbers of seismic events for every energy level were plotted on a logarithmic scale, Figure 7. The size of a marker relates to the number of cells averaged and the colour indicates the average event size. Markers of different type relate to the two major rock mass units contained in the volume.

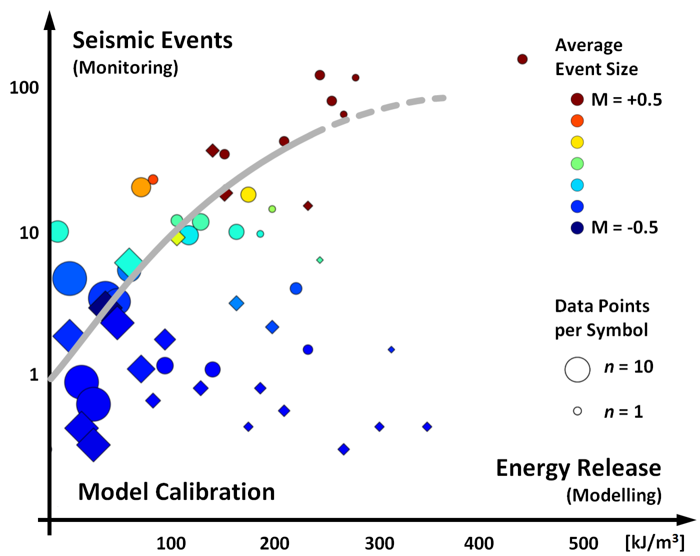

Figure 7. Calibration of seismic event numbers with energy release.

The majority of data points, above 95%, are in the lowest (0 kJ/m^3 to10 kJ/m^3) category, relating to the fact that only part of the grid volume will experience energy release due to mining. These cells are not shown in this plot. As very few data points are collected above 250 kJ/m^3, the confidence in the trend above this level and its use for forecasting is not established.

The calibration is simplified to the centre line indicating the number of seismic events each cell volume can experience.

The author accepts that the resulting plot and its usefulness for other orebodies in the mine is affected by limitations regarding both the modelling approach and the available data:

- Monitoring system location error. The relative position of stations, stopes and events can influence the location data, amplified by the shadowing effect of backfilled stopes.
- Timing of seismic events. The decline in seismicity following a production blast over a few days should ensure that the temporal correlation between model step and events is preserved, but in some cases the data clearly shows ongoing seismic events in subsequent steps, where the modelled energy release only occurs once.
- The different behaviour observed in different rock mass units might be due to their location relative to the mining fronts, and subsequently the energy released, and not to their strength and brittleness.

3.5 Forecasting

Following the calibration, an update of seismic data was received for a period of three months. Several stopes were extracted in this period. The model provided results for these sequence steps, allowing comparison of the data, testing the ability of the model to forecast seismic activity. The same type of plot as in Figure 8 was used to show the predicted seismicity based on energy release,

This test confirms the proposition of a relationship between seismic event numbers and modelled energy release that has the potential to be used as a forecasting tool, Figure 8.

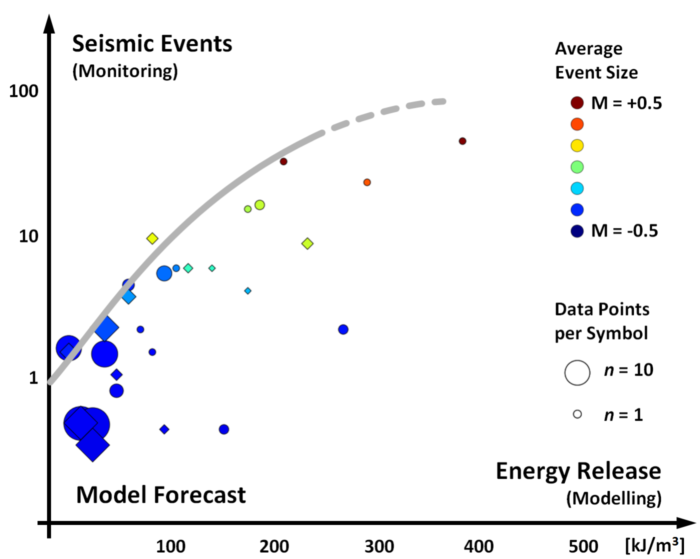

Figure 8. Model forecast for seismic event numbers.

An example of an individual forecasting step for one extracted stope compares energy release from the model step with the seismic events actually incurred in the month. Iso-surfaces of energy release above $10kJ/m^3$ would contain more than one seismic event per 25m volume on average, above $100kJ/m^3$ ten to one hundred seismic events would be expected and also yield higher event sizes on average.

These volumes predicting energy release are shown in Figures 9. The strong directional bias of seismic events located both inside and outside the pillar in the direction of the major principal stress that was observed in the seismic event data is also evident in the model forecast.

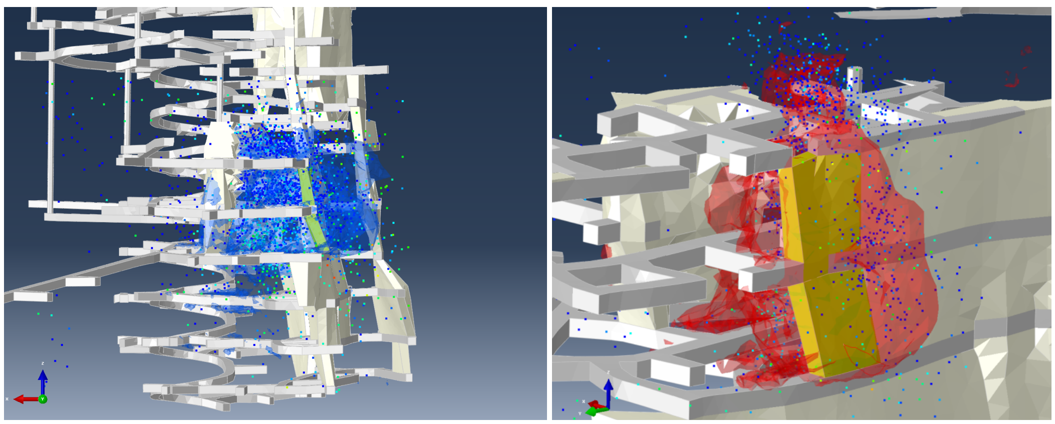

Figure 9. Model forecast of energy release above 10kJ/m3 (blue volume, left) and 100kJ/m3 (red volume, right) and for stope extraction and actual seismic events

This information is available for every mining step in an analysis forecast and can be employed in the mine planning process.

It is important to note that the distribution of the seismicity over time is strongly biased towards the day of extraction of the stopes allowing the modelled energy release to be applied for forecasting if sequencing of the model is done in a large enough number of individual steps. Since larger events occur at low frequencies, a statistical approach is not suitable to identify this risk. Still, the model provides accurate results for stress changes that can be used for evaluation in other methods.

4. Stability in foliated rock mass

Foliated rock mass, consisting of large numbers of parallel joints dividing the intact rock, can be modelled using cohesive elements to represent parallel planes of joints. Although the spacing of joints in real rock mass can be much smaller than can be practically included in the mesh, adopting a smeared approach, such as the Jointed Material Model available in Abaqus/Standard, has the disadvantage of showing very uniform shear deformation across the volume.

4.1 Detailed model with discrete representation of joint planes

Observations for drill holes in this example (typically performed with a bore hole camera or a photograph of the face) show that only a few of the joints in the material actually become active and deform in shear. This localisation can be captured by defining the cohesive elements with strain-softening Mohr-Coulomb plasticity. Once a particular joint plane starts yielding beyond a critical strain, the softening will reduce the yield stress required to cause further deformation. This replicates the mechanism of damage of the in-fill material *in* the joints that activates friction on the joint surfaces. Subsequently the stress changes due to the movement will unload adjacent planes.

A detailed model was built for calibration purposes for a stope spanning 100m, containing both the access development from which the holes were drilled and mined (backfilled) voids above and below. The model contains about 20 parallel planes at 0.5m spacing in the pillar between the stope and the access tunnel, resulting in about 2 million elements, nearly 1 million of which are cohesive elements. The model is shown in Figure 10, with half the volume mesh removed to expose stopes, development and foliation planes.

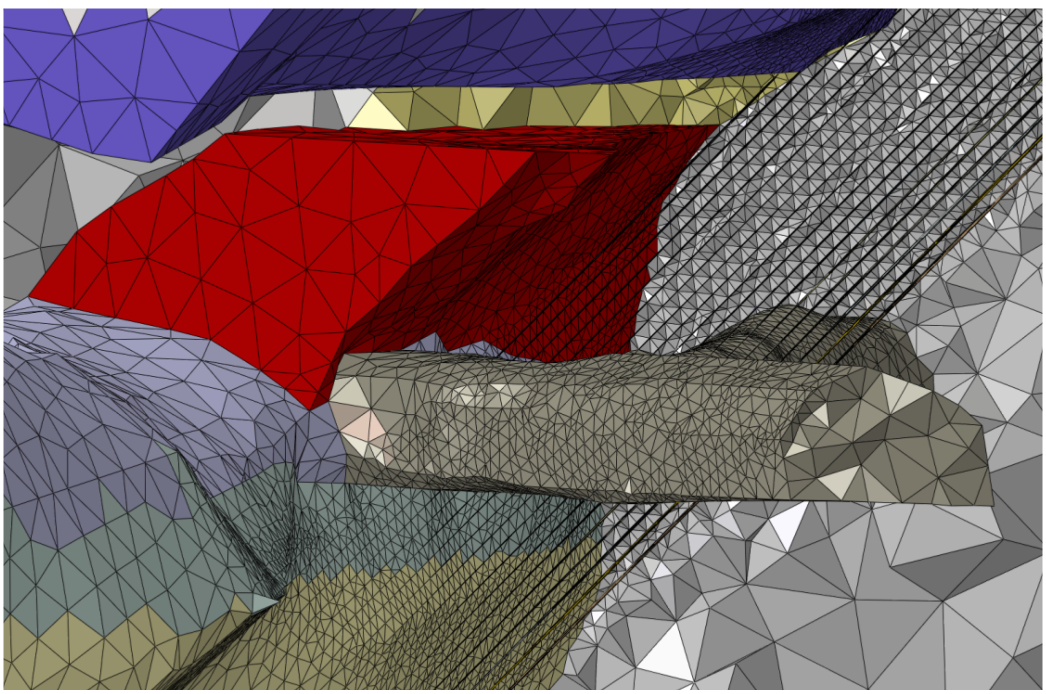

Figure 10. Cut-away view of the finite element model of a stope and access development in foliated ground

The initial conditions for stress in this model and stress boundary conditions are taken from a mine-scale model spanning 8km to account for mining adjacent stopes before the volume shown in red was extracted. The sub-model approach outlined in the previous chapter with displacement driven boundaries would be compromised by the large change of scale with element sizes changing by two magnitudes from the global model.

4.2 Results

The model captures the observed characteristic of rock mass yield and deformation:

- Boreholes located along the drive, crossing the pillar at areas of higher confinement, typically show several joints dislocating. The measurements are captured in categories of shear (below 10mm, 10mm – 20mm and above 20mm). Comparing the cumulative shear displacement along the holes with the displacements on the modelled joints shows the same magnitude of displacement. A view of displacement magnitudes on a vertical section through the pillar together with a photograph of this wall are shown in Figure 11. The inset drawing highlights the mechanism observed. The photograph also shows that the deformation is continuous along the same plane.
- Dilation cracks are visible near the nose of the pillar, indicating that the bulk material is yielding. Concurrently, boreholes near the nose show no deformation on the joints. This is captured both by the bulk plastic strain in volume elements and the near zero displacements on the joints at this location in the model. The displacement magnitudes at the nose and an example borehole at this location are shown in Figure 12

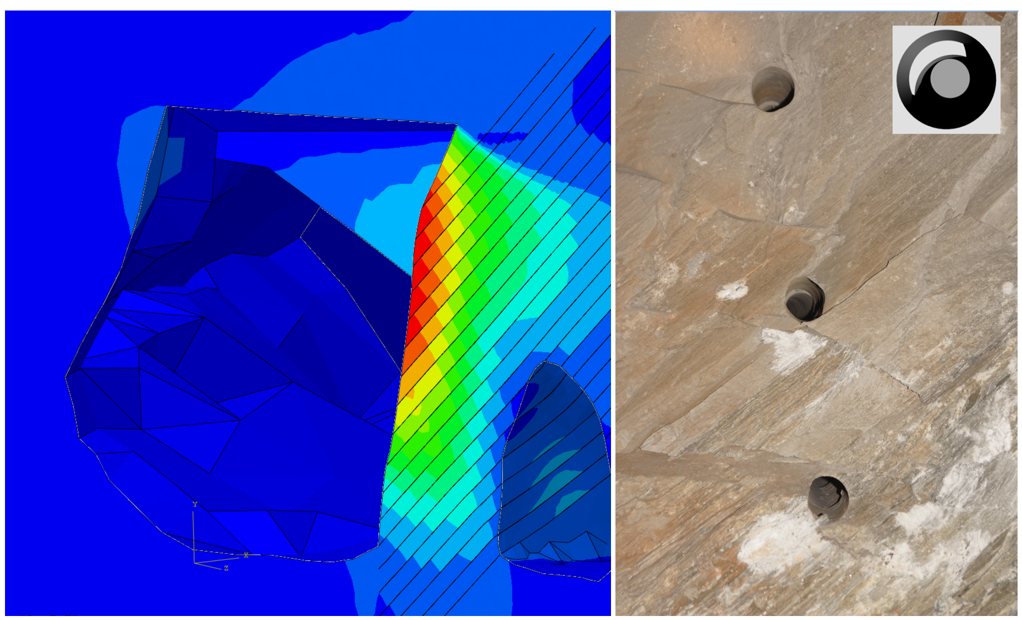

Figure 11. Magnitude of deformation from the Finite Element Model due to stope extraction and observed shearing in drill holes inside the drive

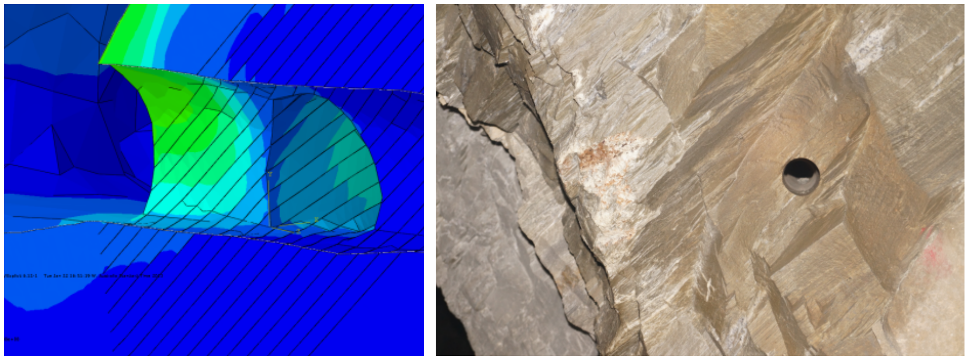

Figure 12. Reduced magnitude of shear on joint planes near the nose and intact drill hole without shear deformation at this location.

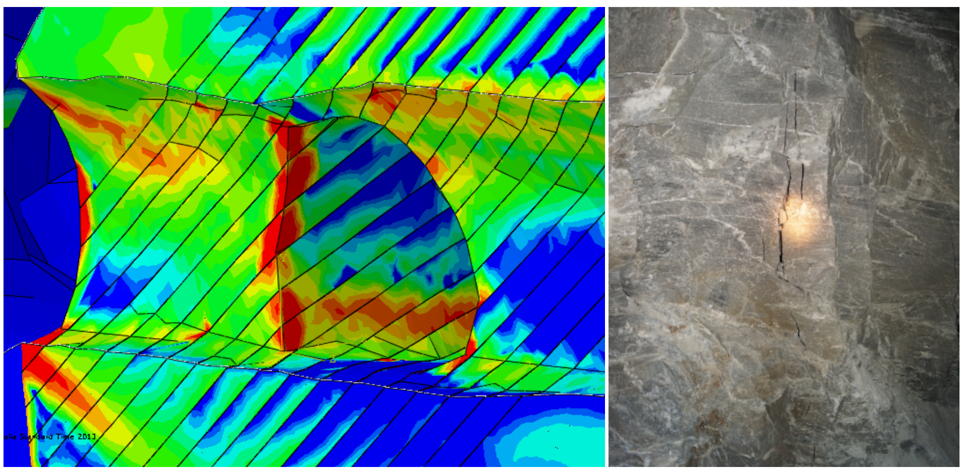

Figure 13. Rock mass yield (bulk plasticity) near the nose which is confirmed by the observed dilation cracks.

4.3 Application

By using several models on different scales and calibration data from global observations, induced stress changes, deformation and rock mass damage the parameters for the different types of rock mass and the joints can be determined within a narrow range of cohesion and friction angle values for each material. This allows the use in forecasting conditions whilst the mine goes deeper, the dip and direction of the orebody changes and excavation spans may have to change due to increase in stress. Working together with geotechnical engineers different designs can be developed and tested in finite element models.

5. References

1. Arndt, S., "Advances in Mining Simulations", In Proceedings of Simulia Customer Conference. London, England. May 18-21, 2009.
2. Arndt, S., Fillery, B., "The Importance of Simulation in Geotechnical and Mining Applications", In Proceedings of Simulia Customer Conference. Barcelona, Spain. May 17-19, 2011.
3. van der Zee, W., Ozan, C., Brudy, M., Holland, M., "3D Geomechanical Modeling of Complex Salt Structures", In Proceedings of Simulia Customer Conference. Barcelona, Spain. May 17-19, 2011.